Photocatalytic Reduction of CO_2 with H_2O on Titanium Oxides Anchored within Micropores of Zeolites: Effects of the Structure of the Active Sites and the Addition of Pt

Masakazu Anpo,* Hiromi Yamashita, Yuichi Ichihashi, Yo Fujii, and Miwa Honda

Department of Applied Chemistry, College of Engineering, Osaka Prefecture University, Gakuen-cho, Sakai, Osaka 593, Japan

Received: August 30, 1996; In Final Form: December 2, 1996[⊗]

Titanium oxide species anchored within the Y-zeolite cavities by an ion-exchange method exhibit a high and unique photocatalytic reactivity for the reduction of CO_2 with H_2O at 328 K with a high selectivity for the formation of CH_3OH in the gas phase. The in situ photoluminescence, ESR, diffuse reflectance absorption, and XAFS (XANES and FT-EXAFS) investigations indicate that the titanium oxide species are highly dispersed within the zeolite cavities and exist in a tetrahedral coordination. The charge transfer excited state of the anchored titanium oxide species plays a significant role in the reduction of CO_2 with H_2O with a high selectivity for the formation of CH_3OH, while the catalysts involving the aggregated octahedrally coordinated titanium oxide species show a high selectivity to produce CH_4, being similar to reactions on the powdered TiO_2 catalysts. The addition of Pt to the anchored titanium oxide catalysts promotes the charge separation which leads to an increase in the CH_4 yields in place of CH_3OH formation.

Introduction

The design of highly efficient and selective photocatalytic systems that work without any loss of energy in the utilization of solar energy through chemical storage is of vital interest. Especially, the efficient photocatalytic reduction of CO_2 with H_2O is one of the most desirable and challenging goals in the research of environmentally friendly catalysts.[1−4] Inoue and Fujishima *et al.*[5] have first reported that HCOOH, HCHO, and a trace amount of CH_3OH are produced by the reduction of CO_2 with H_2O under irradiation of aqueous suspension systems involving a variety of semiconductor powders such as TiO_2 and $SrTiO_3$. The photocatalytic production of CH_4 from CO_2 and H_2O has also been reported by Hemminger *et al.* on the Pt/$SrTiO_3$ catalyst.[6] Although the pioneering works on the photoreduction of CO_2 on semiconductors in aqueous suspension systems were summarized by Halmann[7] and recent work in solid−gas systems were reviewed by Anpo and Yamashita,[8] the efficiency of CO_2 reduction was low when water was used as the reductant, so details of the mechanisms behind this reaction have yet to be clarified.

Recently, several researchers have reported that the photocatalytic reduction of CO_2 with gaseous H_2O proceeded on the powdered TiO_2 at room temperature and only a small amount of CH_4 formation was observed.[1−4,9] Using various types of well-characterized powdered TiO_2 catalysts, we have found that the efficiency of this photoreaction depends strongly on the structure of the photocatalysts. It was found that extremely small TiO_2 particles having large band gaps show the highest efficiency for photocatalytic CH_4 formation.[2] We have concentrated not only on the study of extremely small TiO_2 particles but also on studies of highly dispersed anchored titanium oxides for utilization as photocatalysts.[10] It was found that the highly dispersed titanium oxide catalyst anchored on Vycor glass exhibits a high and characteristic photocatalytic reactivity compared to that of the bulk TiO_2 powder in various photocatalytic reactions.[11−14]

The utilization of the zeolite cavity spaces is also vital to the design and application of highly efficient and selective photocatalytic systems because zeolites offer unique nanoscaled pore reaction fields, an unusual internal surface topology, and ion-exchange capacities. Unique photocatalytic properties which cannot be realized in normal catalytic systems have been observed recently in such modified reaction spaces.[15−17] The titanium oxide species prepared within the zeolite cavities or the zeolite frameworks have recently revealed a unique local structure as well as a high selectivity in the oxidation of organic substances with hydrogen peroxide.[18,19] However, the true chemical nature and reactivities of these titanium oxide species as a photocatalyst are yet little known, especially the photocatalytic reactivity for the reduction of CO_2 with H_2O.

In our present study, the highly dispersed titanium oxides included within zeolite cavities (Ti-oxide/zeolite) were prepared using an ion-exchange method and used as the photocatalyst for the reduction of CO_2 with H_2O at 328 K. The photocatalytic properties of this highly dispersed titanium oxide catalyst were then compared with the properties of the titanium oxide catalysts prepared by an impregnation method as well as with those of the bulk TiO_2 powder catalysts. The characterization of these catalysts by means of in situ photoluminescence, diffuse reflectance absorption, XAFS (XANES and FT-EXAFS), and ESR measurements has been carried out to clarify the characteristics of the photocatalytic reduction of CO_2 with H_2O at 328 K. Special attention has been focused on the relationship between the structure of the titanium oxide species and the reaction selectivity in the photocatalytic reduction of CO_2 with H_2O to form CH_3OH. In addition, the effects of the addition of Pt on the photocatalytic properties have been studied in order to obtain useful and important information required for the design and application of highly active and selective photocatalytic systems for the efficient reduction of CO_2 with H_2O.

Experimental Section

1. Catalysts. The Ti-oxide/Y-zeolite (1.1 wt % as TiO_2) catalyst was prepared by ion exchange with an aqueous titanium ammonium oxalate solution using Y-zeolite samples ($SiO_2/Al_2O_3 = 5.5$) supplied by the TOSOH corporation (ex-Ti-oxide/Y-zeolite). The Pt-loaded ex-Ti-oxide/Y-zeolite catalyst (1.0 wt % as Pt metal) was prepared by impregnating the ex-Ti-

[⊗] Abstract published in *Advance ACS Abstracts,* March 1, 1997.

S1089-5647(96)02696-X CCC: $14.00

oxide/Y-zeolite with an aqueous solution of H_2PtCl_6. Furthermore, two types of Ti-oxide/Y-zeolite catalyst having different Ti contents (1.0 wt % and 10 wt % as TiO_2, respectively) were prepared by impregnating the Y-zeolite with an aqueous solution of titanium ammonium oxalate (imp-Ti-oxide/Y-zeolite). TiO_2 powdered catalysts (JRC-TIO-4: anatase 92%, rutile 8%) were supplied as the standard reference by the Catalysis Society of Japan.[20]

2. Photocatalytic Reaction. The photocatalytic reduction of CO_2 with H_2O was carried out with the catalysts (150 mg involving zeolite) in a quartz cell with a flat bottom (88 mL) connected to a conventional vacuum system (10^{-6} Torr range). Prior to the photoreactions and spectroscopic measurements, the catalysts were degassed at 725 K for 2 h, heated in O_2 at the same temperature for 2 h, and finally evacuated at 475 K to 10^{-6} Torr for 1 h. In the case of the Pt-loaded catalysts, the pretreated catalyst was heated in H_2 at 475 K for 2 h and finally evacuated at the same temperature to 10^{-6} Torr for 1 h. UV irradiation of the catalysts in the presence of CO_2 (24 μmol, 5.5 Torr) and gaseous H_2O (120 μmol) was carried out using a 75 W high-pressure Hg lamp (λ > 280 nm) at 328 K. The reaction products collected in the gas phase were analyzed by gas chromatography.

3. Characterization. The photoluminescence spectra of the catalysts were measured at 77 K using a Shimadzu RF-5000 spectrophotofluorometer. The diffuse reflectance absorption spectra were recorded with a Shimadzu UV-2200A spectrometer at 295 K. The ESR spectra were recorded at 77 K using a JEOL JES-RE2X spectrometer operating in the X-band mode. The XAFS spectra (XANES and EXAFS) were measured at the BL-7C facility of the Photon Factory at the National Laboratory for High-Energy Physics, Tsukuba. The Ti K-edge absorption spectra were recorded in the transmission mode or fluorescence mode at 295 K. The normalized spectra were obtained by a procedure described in previous literature,[21] and the Fourier transformation was performed on k^3-weighted EXAFS oscillations in the range of 3−10 Å^{-1}. The curve fitting of the EXAFS data was carried out by employing the iterative nonlinear least-squares method and the empirical backscattering parameter sets extracted from the shell features of titanium compounds.

Results and Discussion

UV irradiation of the powdered TiO_2 and the Ti-oxide/Y-zeolite catalysts prepared by ion-exchange or impregnation methods in the presence of a mixture of CO_2 and H_2O led to the evolution of CH_4 and CH_3OH in the gas phase at 328 K, as well as trace amounts of CO, C_2H_4, and C_2H_6. The evolution of small amounts of O_2 was also observed. As shown in Figure 1, the rates of these photoformed products increase linearly against the UV-irradiation time, and the reaction immediately stops when irradiation is ceased. The formation of these reaction products was not detected in dark conditions nor with UV irradiation of the zeolites without titanium oxides. These results clearly indicate that the presence of both titanium oxides included within the zeolites as well as UV irradiation are indispensable for the photocatalytic reaction to take place while the reduction of CO_2 with H_2O occurs photocatalytically on the surface of the titanium oxide catalysts.

The photocatalytic reaction rates for the formation of CH_4 and CH_3OH per gram of Ti of the various types of titanium oxides are shown in Figure 2. As shown in Figure 2, depending on the type of titanium oxide catalyst, different photocatalytic reaction rates and different product selectivities can be observed. UV irradiation of the anchored (ex-Ti-oxide/Y-zeolite) catalysts in the presence of a mixture of CO_2 and H_2O leads to the evolution of a large amount of CH_3OH as well as CH_4. Although the addition of Pt to the ex-Ti-oxide/Y-zeolite is effective in increasing the photocatalytic reactivity, only the formation of CH_4 is promoted, accompanied by a decrease in the CH_3OH yields. On the other hand, UV irradiation of the imp-Ti-oxide/Y-zeolite catalysts in the presence of a mixture of CO_2 and H_2O leads to the evolution of CH_4 in the gas phase as the main product. On the imp-Ti-oxide/Y-zeolite catalyst with a small Ti content (1.0 wt % as TiO_2), the formation of a small amount of CH_3OH can be observed, while CH_3OH is not produced on the imp-Ti-oxide/Y-zeolite catalyst with a large Ti content (10.0 wt % as TiO_2). On the powdered TiO_2 catalyst, CH_4 is also mainly produced, but the photocatalytic reaction rate is much smaller than for the titanium oxide catalysts included into the cavities of the Y-zeolites.

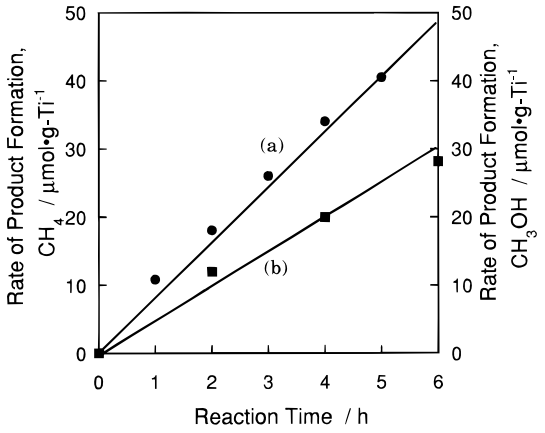

Figure 1. Reaction time profiles of the photocatalytic reduction of CO_2 (24 μmol) with H_2O (120 μmol) to produce CH_4 (a) and CH_3OH (b) on the ex-Ti-oxide/Y-zeolite catalyst.

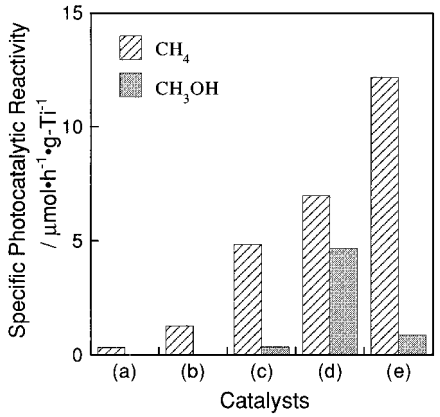

Figure 2. Products distribution of the photocatalytic reduction of CO_2 with H_2O on the anatase TiO_2 powder (a), the imp-Ti-oxide/Y-zeolite (10.0 wt % as TiO_2) (b), the imp-Ti-oxide/Y-zeolite (1.0 wt % as TiO_2) (c), the ex-Ti-oxide/Y-zeolite (d), and the Pt-loaded ex-Ti-oxide/Y-zeolite (e) catalysts.

A comparison of the total rates of CH_4 and CH_3OH formation shows the level of photocatalytic reactivity depending on the type of titanium oxide catalysts to be in the order of Pt-loaded ex-Ti-oxide/Y-zeolite > ex-Ti-oxide/Y-zeolite > imp-Ti-oxide/Y-zeolite (1.0 wt % as TiO_2) > imp-Ti-oxide/Y-zeolite (10.0 wt % as TiO_2) > TiO_2 powders. Among these photocatalysts, the ex-Ti-oxide/Y-zeolite exhibits the highest rate of CH_3OH formation, while the highest rate of CH_4 formation can be observed with the Pt-loaded ex-Ti-oxide/Y-zeolite.

From Figure 2, it is clear that the photocatalytic reaction rate and selectivity for the formation of CH_3OH strongly depend on the type of catalyst. Of special interest is the comparison of the photocatalytic reaction rates of the Ti-oxide/Y-zeolite

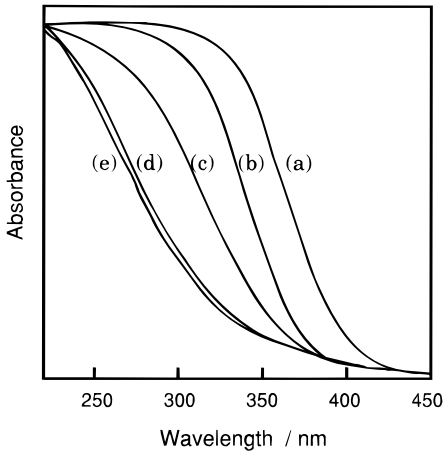

Figure 3. Diffuse reflectance absorption spectra of the anatase TiO_2 powder (a), the imp-Ti-oxide/Y-zeolite (10.0 wt % as TiO_2) (b), the imp-Ti-oxide/Y-zeolite (1.0 wt % as TiO_2) (c), the ex-Ti-oxide/Y-zeolite (d), and the Pt-loaded ex-Ti-oxide/Y-zeolite (e) catalysts.

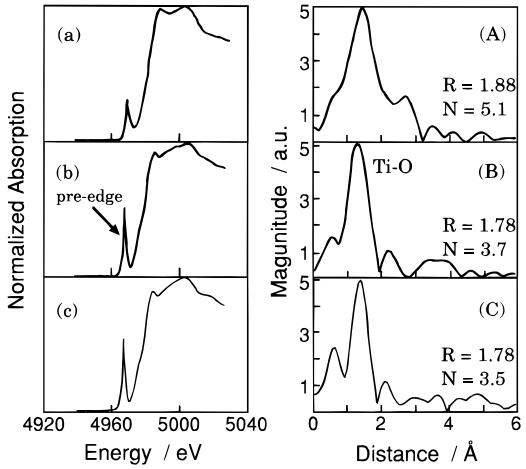

Figure 4. XANES (a−c) and FT-EXAFS (A−C) spectra of the imp-Ti-oxide/Y-zeolite (1.0 wt % as TiO_2) (a, A), the ex-Ti-oxide/Y-zeolite (b, B), and the Pt-loaded ex-Ti-oxide/Y-zeolite (c, C) catalysts. Coordination numbers (N) and atomic distances (R, Å) obtained from curve-fitting analysis of EXAFS spectra are shown.

catalysts with that of the widely used bulk TiO_2 powdered catalyst. It can be seen that the photocatalytic reaction rates of the Ti-oxide/Y-zeolite catalysts corresponding to the reaction time which have been normalized for the unit gram of Ti in the catalysts are much higher than those of the bulk TiO_2 catalysts. The ex-Ti-oxide/Y-zeolite catalyst exhibits a high reactivity and a high selectivity for the formation of CH_3OH, while the formation of CH_4 was found to be the major reaction on the bulk TiO_2 catalyst as well as on the imp-Ti-oxide/Y-zeolite catalyst and Pt-loaded catalyst. Thus, the results obtained with the ex-Ti-oxide/Y-zeolites clearly show the large difference in selectivity as well as the photocatalytic reaction rates with the imp-Ti-oxide/Y-zeolite, Pt-loaded catalysts, and the bulk TiO_2 catalyst.

Figure 3 shows the absorption spectra of the Ti-oxide/Y-zeolite and bulk TiO_2 catalysts measured by the UV diffuse reflectance method. The ex-Ti-oxide/Y-zeolite catalyst exhibits absorption bands in the wavelength regions of 270−330 nm, shifting into shorter wavelength regions as compared to those of the bulk TiO_2 catalyst. Such a shift to the shorter wavelength in the absorption band of titanium oxides can be attributed to the size quantization effect due to the presence of extremely small Ti-oxide particles and/or the presence of highly unsaturated Ti-oxide species having a tetrahedral coordination.[22−24] The Pt-loaded catalyst exhibits the same spectra, indicating that the local structure of the anchored titanium oxide is not changed by Pt loading. On the other hand, the imp-Ti-oxide/Y-zeolite catalysts exhibit absorption bands in the wavelength regions of 330−370 nm, their intensity increasing with an increase in the content of Ti. A significant shift to the shorter wavelength in the absorption band can be observed with the ex-Ti-oxide/Y-zeolite catalyst, clearly suggesting that the dispersion of the Ti-oxide species on this catalyst is higher than on the catalysts prepared by impregnation methods. Thus, a clear relationship can be seen between the reactivity for the photocatalytic reduction of CO_2 with H_2O, especially to form CH_3OH, and the magnitude of the shift toward the shorter wavelength of these catalysts.

Figure 4 shows the XANES spectra of the Ti-oxide/Y-zeolite catalysts. The XANES spectra of the Ti-oxide catalyst at the Ti K-edge show several well-defined preedge peaks which are related to the local structures surrounding the Ti atom. These relative intensities of the preedge peaks provide useful information on the coordination number surrounding the Ti atom.[24−27] As shown in Figure 4b, the ex-Ti-oxide/Y-zeolite catalyst exhibits an intense single preedge peak. Because tetrahedrally coordinated Ti such as $Ti(OPr^i)_4$ was found to exhibit an intense single preedge peak due to the lack of an inversion center in the regular tetrahedron structure, the observation of this intense single preedge peak indicates that the titanium oxide species in the ex-Ti-oxide/Y-zeolite catalyst has a tetrahedral coordination. The Pt-loaded catalyst (Figure 4c) also exhibits the same preedge peak, indicating that Pt loading does not lead to any change in the local structure of the anchored titanium oxide. As can be seen in Figure 4a, for the imp-Ti-oxide/Y-zeolite catalyst having a small Ti content, the single characteristic preedge peak is rather weak, indicating that the catalyst consists of a mixture of tetrahedrally and octahedrally coordinated titanium oxide species. On the other hand, the imp-Ti-oxide/Y-zeolite catalyst having a high Ti content exhibits three characteristic weak preedge peaks. Because these characteristic small preedge peaks are attributed to the transitions from the 1s core level of Ti to three different kinds of molecular orbitals ($^1t_{1g}$, $^2t_{2g}$, and ^3e_g) of anatase TiO_2, these observations indicate the presence of the crystalline anatase TiO_2 in the imp-Ti-oxide/Y-zeolite catalysts.

Figure 4 also shows the FT-EXAFS spectra of the catalysts, and all data are given without corrections for phase shifts. All of the catalysts investigated in the present study exhibit a strong peak at around 1.6 Å (uncorrected for the phase shift) which can be assigned to the neighboring oxygen atoms (Ti−O). The ex-Ti-oxide/Y-zeolite (Figure 4B) and Pt-loaded catalysts (Figure 4C) exhibit only Ti−O peaks, indicating the presence of the isolated titanium oxide species on these catalysts. From the results obtained by the curve-fitting analysis of the EXAFS spectra, it was found that the ex-Ti-oxide/Y-zeolite catalyst consists of 4-coordinate titanium ions with a coordination number of 3.7 and an atomic distance of 1.78 Å. This atomic distance is similar to those observed with tetrahedrally coordinated titanium oxide which is included within the zeolite framework.[25−27]

As shown in Figure 4A, the imp-Ti-oxide/Y-zeolite catalysts exhibit an intense peak at around 2.7 Å. This peak can be assigned to the neighboring titanium atoms (Ti−O−Ti) as well as to the Ti−O peak, indicating the aggregation of the titanium oxide species in these catalysts. Results of the coordination number of 5.8 and an atomic distance of 1.93 Å for the imp-Ti-oxide/Y-zeolite (10.0 wt % as TiO_2) obtained by the curve-fitting analysis of the EXAFS spectra and also the coordination number of 5.1 and an atomic distance of 1.88 Å for the imp-Ti-oxide/Y-zeolite (1.1 wt % as TiO_2) suggest the presence of

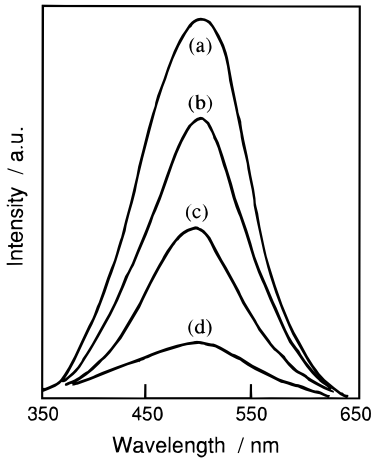

Figure 5. Photoluminescence spectrum of the ex-Ti-oxide/Y-zeolite catalyst (a) and the effects of the addition of CO_2 and H_2O (b, c) and the loading of Pt (d) on the photoluminescence spectrum. Measured at 77 K, excitation at 290 nm, amount of added CO_2 (b), 8.5 μmol g^{-1}; amount of added H_2O (c), 2.9 μmol g^{-1}.

an aggregated octahedral titanium oxide species with the impregnated catalysts.

These XANES and FT-EXAFS investigations indicate that the ex-Ti-oxide/Y-zeolite catalyst involves only the well-isolated tetrahedral Ti-oxide species whose local structure is maintained even after Pt loading, while the imp-Ti-oxide/Y-zeolite catalyst involves the aggregated octahedral Ti-oxide species. Figure 5 shows that the ex-Ti-oxide/Y-zeolite catalyst exhibits a photoluminescence spectrum at around 490 nm by excitation at around 290 nm at 77 K. The observed photoluminescence and absorption bands are in good agreement with those previously observed with the highly dispersed tetrahedrally coordinated titanium oxides prepared in silica matrices, where the absorption of UV light at around 280 nm brings about an electron transfer from the lattice oxygen (O_l^{2-}) to the titanium ion (Ti^{4+}) to form a charge transfer excited state.[28,29] We can therefore conclude that the observed photoluminescence spectrum is attributed to the radiative decay process from the charge transfer excited state formed in this way to the ground state of the highly dispersed titanium oxide species having a tetrahedral coordination as shown in the following scheme. The lifetime of the charge

$$(Ti^{4+}-O^{2-}) \underset{h\nu'}{\overset{h\nu}{\rightleftharpoons}} (Ti^{3+}-O^{-})^*$$

transfer excited state of the ex-Ti-oxide/Y-zeolite catalyst was determined to be 54 μs, being much longer than that of the TiO_2 powders (nanosecond order). Such a long lifetime of the charge transfer excited state is well-associated with the presence of highly dispersed homogeneous tetrahedral titanium oxide species. On the other hand, the imp-Ti-oxide/Y-zeolite catalysts did not exhibit any photoluminescence spectra. Thus, these results clearly indicate that the ex-Ti-oxide/Y-zeolite catalyst consists of the highly dispersed isolated tetrahedral titanium oxide species, while the imp-Ti-oxide/Y-zeolite catalysts involve the aggregated octahedral titanium oxide species which do not exhibit any photoluminescence spectra, being in good agreement with results obtained by XAFS investigations.

As shown in Figure 5, the addition of H_2O or CO_2 molecules onto the ex-Ti-oxide/Y-zeolite catalyst leads to the efficient quenching of the photoluminescence with different efficiencies. The lifetime of the charge transfer excited state was also found to be shortened by the addition of CO_2 or H_2O, its extent depending on the amount of added gasses. Such an efficient quenching of the photoluminescence with CO_2 or H_2O suggests not only that tetrahedrally coordinated titanium oxide species locate at positions accessible to the added CO_2 or H_2O but also that added CO_2 or H_2O interacts and/or reacts with the anchored titanium oxide species in both its ground and excited states. The addition of CO_2 was less effective for the quenching of the photoluminescence in their intensities and lifetimes than those observed by the addition of H_2O, indicating that the interaction of CO_2 with the titanium oxide species is weaker than that of H_2O.

Furthermore, as shown in Figure 5, Pt loading onto the ex-TiO_2/Y-zeolite catalyst leads to the efficient quenching of the photoluminescence, accompanied by the shortening of its lifetime. Because the results obtained by the EXAFS and diffuse reflectance absorption measurements indicated that the local structure of the titanium oxide species in the ex-TiO_2/Y-zeolite was not altered by Pt loading, the effective quenching of the photoluminescence can be attributed to the electron transfer from the photoexcited titanium oxide species to Pt metals which exist in the neighborhood of the titanium oxide species. The electrons are easily transferred from the charge transfer excited state of titanium oxide species, electron-hole pair state of $(Ti^{3+}-O^{-})^*$, to the Pt moieties while the holes remain in the titanium oxide species, resulting in the charge separation of electrons and holes from the photoformed electron-hole pair states. As result, on the Pt-loaded ex-Ti-oxide/Y-zeolite catalyst, photocatalytic reactions, which proceed in the same manner as on bulk TiO_2 catalysts, become predominant, and the reduction reaction by electrons and the oxidation reaction by holes occur separately from each other on different sites.

In order to obtain detailed information on the mechanisms behind these photocatalytic reactions, various mixtures of the reactant gasses, *i.e.*, CO and H_2O, CO_2 and H_2, as well as CO_2 alone were also investigated. In the case of CO_2 alone, no reaction occurred, indicating that the presence of H_2O is indispensable for the reaction. Furthermore, in the photocatalytic reaction of the CO_2 and H_2 mixture, no products were observed with the Ti-oxide/Y-zeolite catalysts. These results indicate that the photocatalytic decomposition of H_2O is involved in the photocatalytic reduction of CO_2 on Ti-oxide/Y-zeolites. On the other hand, CH_4 and CH_3OH were mainly produced from the CO and H_2O mixture as well as from the CO_2 and H_2O mixture. We found that CO is an intermediate species in the reaction of the CO_2 and H_2O mixture.

UV irradiation of the anchored titanium oxide catalyst in the presence of CO_2 and H_2O at 77 K led to the appearance of ESR signals due to the Ti^{3+} ions, H atoms, and carbon radicals.[1,4] These ESR signals increased in intensity with the UV irradiation time at 77 K and were found to disappear once the temperature of the cell was raised to 275 K. In this system the formation of CH_4 was detected as a product, though the amount was very small as compared with that of the photoreaction. The relative intensities of these ESR signals strongly depended on the amount of CO_2 and H_2O on the catalyst, the intensity of the H atoms increasing with an increase in the amount of H_2O while the intensity of the Ti^{3+} ions decreased. From these results the reaction mechanism in the photocatalytic reduction of CO_2 with H_2O on the highly dispersed titanium oxide catalyst can be proposed as follows. CO_2 and H_2O molecules interact with the excited state of the photoinduced $(Ti^{3+}-O^{-})^*$ species, and the reduction of CO_2 and the decomposition of H_2O proceed competitively. Furthermore, H atoms and $OH^{\bullet}$ radicals are formed from H_2O, and these radicals react with the carbon species formed from CO_2 to produce CH_4 and CH_3OH. The amounts of the adsorbed reactant and of the desorbed products strongly depend on the nature of the catalysts.

Conclusions

It should be emphasized that a high photocatalytic efficiency and selectivity for the formation of CH_3OH in the photocatalytic reduction of CO_2 with H_2O was achieved with the ex-Ti-oxide/Y-zeolite catalyst having highly dispersed isolated tetrahedral titanium oxide species, while the formation of CH_4 in the photocatalytic reduction of CO_2 with H_2O was found to proceed on the bulk TiO_2 catalysts and on the imp-Ti-oxide/Y-zeolite catalysts involving aggregated octahedrally coordinated titanium oxide species. On the isolated tetrahedral titanium oxide species, the charge transfer excited complexes of the oxides, $(Ti^{3+}-O^-)^*$, are formed under UV irradiation. Within their lifetimes the electron transfer from the electron-trapped center, Ti^{3+}, into H^+ and CO_2 takes place to form H atoms, CO, and finally carbon radicals, and simultaneously, the electron transfer from the OH^- into the trapped hole center, O^-, occurs to form $OH^\bullet$ radicals. The reaction between these radicals leads to the formation of CH_3OH as well as CH_4.

On the other hand, with the aggregated or bulk TiO_2 catalysts, the photoformed holes and electrons rapidly separate from each other with large spaces between the holes and electrons, thus preventing the reaction between the carbon radicals and $OH^\bullet$ radicals on the same active sites, resulting in the formation of CH_4 due to the reaction between the H atoms and carbon radicals formed at the electron-trapped center. In the case of the Pt-loaded ex-Ti-oxide/Y-zeolites, CH_4 was mainly formed in place of CH_3OH, although an isolated tetrahedral titanium oxide species exists in this catalyst. The efficient quenching of the photoluminescence by Pt loading and the efficient electron transfer from the electron-trapped center, Ti^{3+}, into the Pt metals promote the charge separation which results in preventing the reaction between carbon radicals and $OH^\bullet$ radicals formed on different sites to form CH_3OH while promoting the reaction between the carbon radicals and H atoms formed on the Pt metals to form CH_4.

Although the study of the detailed mechanisms involving such a local charge separation observed on the highly dispersed titanium oxide catalysts will be the subject of our future work, the present study clearly demonstrates that the titanium oxide species anchored within zeolite cavities are promising candidates for new and applicable photocatalysts for the reduction of CO_2 with H_2O to form CH_3OH selectively.

Acknowledgment. The present work has been supported in part by the Grant-in-Aid on Priority-Area-Research on "Photoreaction Dynamics" (06239110), "Catalytic Chemistry of Unique Reaction Fields" (08232271), and International Joint Project Research (07044162) of the Ministry of Education, Science, Sports, and Culture of Japan. M. Anpo is much indebted to Osaka Prefecture for the Special Project Research and Tokyo Ohka Foundation for their financial support as well as to the Tosoh Corp. for kindly providing the Y-zeolite samples. This work was also sponsored by New Energy and Industrial Technology Development Organization (NEDO)/Research Institute of Innovaite Technology for the Earth (RITE). The authors thank the referees for useful comments.

References and Notes

(1) Anpo, M.; Chiba, K. *J. Mol. Catal.* **1992**, *74*, 207.
(2) Yamashita, H.; Nishiguchi, H.; Kamada, N.; Anpo, M.; Teraoka, Y.; Hatano, H.; Ehara, S.; Kikui, K.; Palmisano, L.; Sclafani, A.; Schiavello, M.; Fox, M. A.; *Res. Chem. Intermed.* **1994**, *20*, 815.
(3) Yamashita, H.; Kamada, N.; He, H.; Tanaka, K.; Ehara, S.; Anpo, M. *Chem. Lett.* **1994**, 855.
(4) Anpo, M.; Yamashita, H.; Ichihashi, Y.; Ehara, S. *J. Electroanal. Chem.* **1995**, *396*, 21.
(5) Inoue, T.; Fujishima, A.; Konishi, S.; Honda, K. *Nature* **1979**, *277*, 637.
(6) Hemminger, J. C.; Carr, R.; Somorjai, G. A. *Chem. Phys. Lett.* **1978**, *57*, 100.
(7) Halmann, M. In *Energy Resources through Photochemistry and Catalysis*; Grätzel, M., Ed.; Academic Press: New York, 1983, p 507.
(8) Anpo, M.; Yamashita, H. In *Heterogeneouse Photocatalysis*; Schiavello, M., Ed.; John Wiley & Sons: Chichester, U.K., in press.
(9) Saladin, F.; Forss, L.; Kamber, I. *J. Chem. Soc., Chem. Commun.* **1995**, 533.
(10) Anpo, M.; Yamashita, H. In *Surface Photochemistry*; Anpo, M., Ed.; John Wiley & Sons: Chichester, U.K., 1996, p 117.
(11) Anpo, M.; Aikawa, N.; Kubokawa, Y. *J. Chem. Soc., Chem. Commun.* **1984**, 644.
(12) Anpo, M.; Aikawa, N.; Kubokawa, Y.; Che, M.; Louis, C.; Giamello, E. *J. Phys. Chem.* **1985**, *89*, 5017.
(13) Anpo, M.; Aikawa, N.; Kubokawa, Y.; Che, M.; Louis, C.; Giamello, E. *J. Phys. Chem.* **1985**, *89*, 5689.
(14) Anpo, M.; Shima, T.; Fujii, T.; Che, M. *Chem. Lett.* **1987**, 65.
(15) Anpo, M.; Matsuoka, M.; Shioya, Y.; Yamashita, H.; Giamello, E.; Morterra, C.; Che, M.; Patterson, H. H.; Webber, S.; Ouellette, S.; Fox, M. A. *J. Phys. Chem.* **1994**, *98*, 5744.
(16) Yamashita, H.; Matsuoka, M.; Tsuji, K.; Shioya, Y.; Anpo, M.; Che, M. *J. Phys. Chem.* **1996**, *100*, 397.
(17) Matsuoka, M.; Matsuda, E.; Tsuji, K.; Yamashita, H.; Anpo, M. *J. Mol. Catal. A: Chem.* **1996**, *107*, 399.
(18) Tatsumi, T.; Nakamura, M.; Negishi, S.; Tominaga, H. *J. Chem. Soc., Chem. Commun.* **1990**, 476.
(19) Reddy, J. S.; Kumar, R. *J. Catal.* **1991**, *130*, 440.
(20) Murakami, Y. In *Preparation Catalysts III*; Catalysis Society of Japan, Tokyo, 1983; p 775.
(21) Tanaka, T.; Yamashita, H.; Tsuchitani, R.; Funabiki, T.; Yoshida, S. *J. Chem. Soc., Faraday Trans. 1* **1988**, *84*, 2987.
(22) Anpo, M.; Nakaya, H.; Kodama, S.; Kubokawa, Y.; Domen, K.; Onishi, T. *J. Phys. Chem.* **1986**, *90*, 1633.
(23) Liu, X.; Iu K.; Thomas, J. K. *J. Chem. Soc., Faraday Trans.* **1993**, *89*, 1861.
(24) Yamashita, H.; Ichihashi, Y.; Harada, M.; Stewart, G.; Fox, M. A.; Anpo, M. *J. Catal.* **1996**, *158*, 97.
(25) Liu, Z.; Davis, R. J. *J. Phys. Chem.* **1994**, *98*, 1253.
(26) Bordiga, S.; Coluccia, S.; Lamberti, C.; Marchese, L.; Zecchina, A.; Boscherini, F.; Buffa, F.; Genoni, F.; Leofanti, G.; Petrini, G.; Vlaic, G. *J. Phys. Chem.* **1994**, *98*, 1253.
(27) Bonneviot, L.; On, D. T.; Lopez, A. *J. Chem. Soc., Chem. Commun.* **1993**, 685.
(28) Yamashita, H.; Ichihashi, Y.; Anpo, M.; Hashimoto, M.; Louis, C.; Chem, M. *J. Phys. Chem.* **1996**, *100*, 16041.
(29) Anpo, M. *Res. Chem. Intermed.* **1989**, *9*, 67.